Mechanistic dichotomy in the gas-phase addition of NO3 to polycyclic aromatic hydrocarbons: Theoretical study

Mechanistic dichotomy in the gas-phase addition of $NO_3^{\bullet}$ to Polycyclic Aromatic Hydrocarbons. Theoretical study.

Giovanni Ghigo,* Andrea Maranzana, Glauco Tonachini

Dipartimento di Chimica, Università di Torino, Via Giuria 7, I-10125 Torino, Italy

Abstract. The gas-phase addition mechanism of the radical NO_3 (an important tropospheric nocturnal oxidizing species) to some selected polycyclic aromatic hydrocarbons (important pollutants of the troposphere) has been computationally analysed. Scope of this work is to verify whether, along with the simple radical addition to the π aromatic system, the reaction can take place through a different mechanism. This alternative pathway consists in an Electron Transfer from the aromatics to NO_3, thus generating an aromatic radical-cation and a nitrate anion. The coulomb attraction should finally bind the two species and generate the radical adduct without any (electronic) energy barrier. The CASPT2 results show that, while benzene and naphthalene react with NO_3 through a plain radical mechanism, anthracene reacts by a mechanism with a partial Electron Transfer character, and pentacene reacts with a sort of *inner-sphere* Electron Transfer pathway. These results concur to explain the high reactivity of NO_3 with larger PAHs whose ionization energy is below 7 eV and could be important in studies of environmental PAH oxidative degradation.

Keywords: PAH, NO_3, Benzene, Naphthalene, Anthracene, Pentacene, Electron Transfer, CASPT2, State Average, B3LYP.

Proposed running title: Dichotomy in the addition of NO_3 to PAHs

* corresponding author. e-mail: giovanni.ghigo@unito.it phone: ++39-011-670-7872 fax: ++39-011-670-7591

Introduction.

Polycyclic aromatic hydrocarbons (PAHs) and their oxidized derivatives are ubiquitous and toxic environmental pollutants present in the troposphere.[1,2] They are emitted during incomplete combustion of fossil fuels[3] and biomass.[4-6] PAHs can undergo oxidation, and functionalization in general, during both combustion and their subsequent transport in the troposphere. Because some of the oxidized PAH derivatives are of concern for human health,[7-11] it is worthwhile to investigate the mechanistic details of these processes. The reaction with the NO_3 radical, known to play in general a significant role in night time tropospheric chemistry,[12] have importance in contributing to nocturnal PAH loss pathways. Theoretical investigations as the present one can be complementary to experimental studies, and usefully compared to them. As examples of papers related to the present one, we report that on benzene[13] or naphthalene[14] plus NO_3 by Qu, Zhang, and Wang, that on benzene and naphthalene by Ghigo *et al.*[15], on anthracene and phenantrene by Maranzana *et al.*[16] and on fluoranthene and pyrene by Wang *et al.*[17] All these studies were mainly focused on the fate of the nitroxy-aryl radical formed by addition of NO_3 radical to some selected positions of the PAHs. In all cases the details of the formation of these radical adducts were not deeply explored because the transition structures leading to them were not identified (*i.e.* the potential energy surface was found attractive at all C-O distances[13,14]), or because their energies were found to be lower than that of the isolated reactants because of some complex.[15,17] A strong dependence of the energy barriers on the theoretical method was also observed.[15]

The NO_3 radical is a quite strong oxidizing specie being its Electron Affinity 3.937 eV[18] while PAHs are species that can be oxidized to radical cations. The Ionization Energy (IE) for benzene (not strictly a PAH but that cannot be missing in this study because the simplest aromatic hydrocarbon can be seen as a reference system) is 9.24.[19] The IE for some selected acene PAHs (Scheme 1) are: eV for benzene C_6H_6, 8.14 eV for naphthalene $C_{10}H_8$,[20] 7.44 eV for anthracene $C_{14}H_{10}$,[21] and 6.93 eV for pentacene $C_{22}H_{14}$.[22] These values suggested that the reaction of NO_3 with some of the larger PAHs may show characteristics different from simple radical addition to a π system (Scheme 2, "RADICAL PATHWAY").

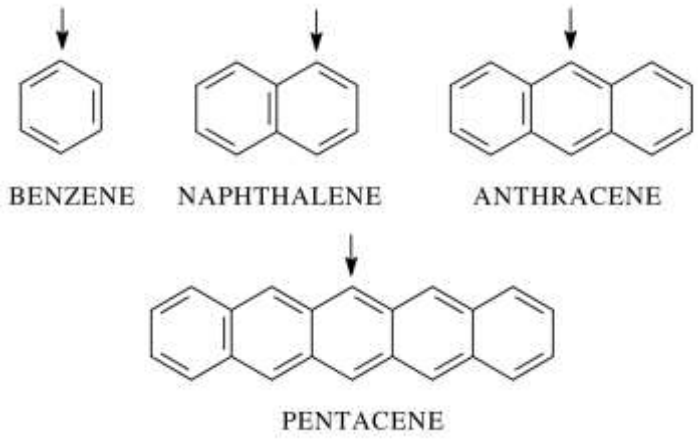

Scheme 1. The Polycyclic Aromatic Hydrocarbons subject of this study. Arrows indicate where NO_3 most probably attacks.

We want to assess whether the thermal reaction, at least in some cases, may take place through an Electron Transfer (ET, hereafter) from the PAH to the NO_3 radical forming a PAH radical-cation and a nitrate anion, NO_3^- (Scheme 2, "ELECTRON TRANSFER PATHWAY"). The strong coulomb attraction between these two species would be at the origin of the lack of an energy barrier. In any case, the resulting adduct Ar-ONO_2 (Scheme 2, right structure) (would be the very same radical, whichever the mechanism.

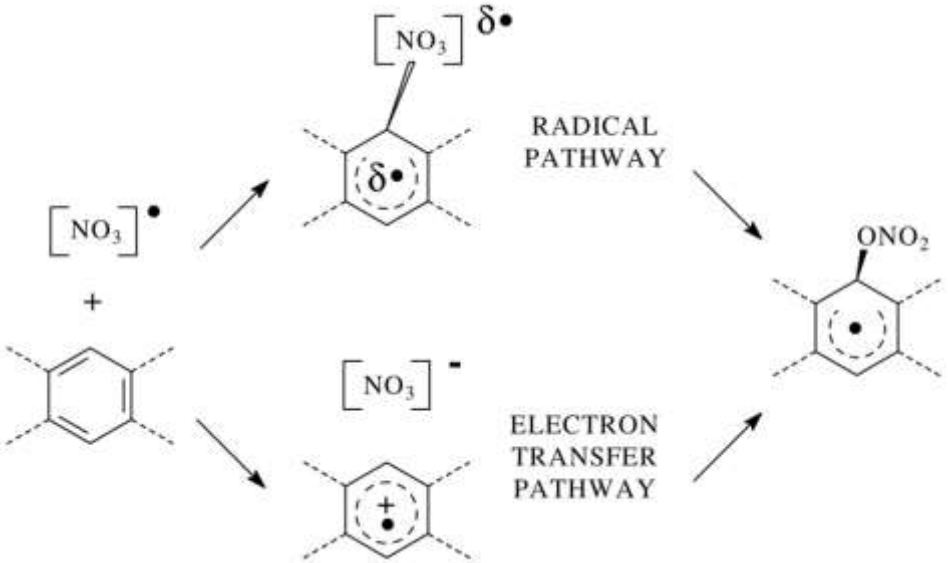

Scheme 2. The "RADICAL" and "ELECTRON-TRANSFER" pathways to the radical adduct Ar-ONO_2 (right) generated by the attack of NO_3 to an aromatics.

The only study where NO_3 radical has been found to react with aromatics by ET are relative to the oxidation of anisole, acetophenone and phenylacetic acid in water.[23] In another case the oxidation by NO_3 of toluene, ethylbenzene and cumene in water and acetonitrile was not certain.[24] We have not found any case

involving larger aromatics.

Scope of this work is not to calculate accurate energy barriers but to explore whether the reaction between NO_3 and the PAHs listed above (Scheme 1) can take place through an ET mechanism as an alternative to the commonly accepted radical process. Clearly the presence of a solvent will strongly affect the choice between the two mechanisms but here we limit the study to the gas-phase reaction because we are specifically interested to tropospheric environment. To verify this hypothesis, we will calculate the adiabatic[25,26] CASPT2 energies of the ground state and of some excited states as a function of the distance between the C and O atoms that will form the bond in the radical adduct Ar-ONO_2. Indeed, we use the same computational approach followed in the study of the heterolytic *versus* homolytic dissociation of LiF[27-29] and NaCl.[30,31] The energy trends, the electronic natures of all states and the electronic charges of the NO_3 moiety will be analyzed in order to collect indications on the two alternative pathways for the attack of NO_3 to the PAHs. Despite the necessary inclusion of some excited states, we will focus our attention on the ground state. In particular, we will look whether this state assumes an ET character when NO_3 is in proximity of the aromatics; character that is expected to be found in one excited state when NO_3 is far from the PAH. This is what clearly happens in the cases of LiF[27-29] where when the atoms are at large distances they show almost null atomic charges (describing two radical atoms) that suddenly raise to +/- 0.88 as they reduce the distance below 13 Å. This is a clear evidence of the formation of two ions through an ET (although the atomic charges are not fully unitary) even if the EA of F (or Cl) is smaller than the IE of Li (or Na).

Theoretical method.

Because the ET is expected to corresponds to an excited state at large C-O distances, the study has been performed by a Multi-Configurational Self-Consistent-Field method (MC-SCF) with the State Average (SA) approach within the Complete-Active-Space Self-Consistent-Field (CASSCF) theory.[32-34] This method allows the correct description of all electronic states for which the inclusion of the suitable Molecular Orbitals (MOs) in the Active Space (AS) is essential. The dynamic electron correlation has then been included in the total energy through the CASPT2 method.[35-37] This is a second order perturbation method based on a multiconfigurational reference wavefunction obtained at the

CASSCF. CASPT2 has been validated in many different studies on properties, reactivity, photophysics and photochemistry of organic molecules.[38-40]

The number of states to be included in the SA calculations, the Molecular Orbitals to be included in the AS and the Basis Set have been defined as a compromise between a reasonable accuracy and the computational affordability for the larger PAH.

The number of states included in the SA was however the minimum required to include the ET state at long C-O distance.

The basis was chosen considering that NO_3 must be reasonably well described both as radical and as anion, therefore, we used the Aug-cc-pVDZ.[41] For the PAHs the same basis set without diffuse functions (cc-pVDZ) was considered to be large enough. This combination of basis sets has been labelled (A)DZ.

As a general rule, the AS should contain all valence MOs and the minimal must contains the HOMO, the LUMO and the SOMO (as in the case of NO_3).[42] Non-physical CASPT2 energy trends and low Reference Weights are also indications on how to extend the AS.[43] In an aromatic system this means the inclusion of all orbitals with π character. However, because of the large dimension of the system object of our study and despite the use of symmetry for all cases but naphthalene (see later) this condition cannot be totally fulfilled. Despite its small dimensions, it is quite hard to model computationally the NO_3 radical in an accurate way (by contrast, it is easy to model satisfactorily the closed shell NO_3 anion).[44-46] Therefore, the construction of the AS first started performing some tests on the electron affinity and on the lowest excited states of NO_3. These tests suggested that a reasonable compromise between accuracy and computational affordability was defined as 9 electrons in 6 MOs (denoted as 9,6). When possible, this AS will be enlarged to (11,7). The active space for the PAHs was initially defined as 4 electron in 4 MOs including the two highest occupied and the two lowest unoccupied π orbitals (4,4). This choice defines a (13,10) AS. Following the indications reported in the Warning section of the CASPT2 output, this active space will be enlarged by different extent and type of MOs for each case as much as computationally affordable. Pictures of the active MOs for each species are reported in the Supplementary Material.

The dimensions of the systems require to limit the study to single point CASPT2/(A)DZ calculations. These have been performed on geometries obtained by DFT[47-49] with the functional B3LYP[50,51] and (A)DZ basis set. This approach

has been chosen because known to give good geometries and because used in the CBS-Q3[52] composed method which we used for some selected key structures for sake of comparison with the DFT and CASPT2 values. In order to be able to afford the calculations for the larger PAHs we took advantage of the C_s symmetry whenever possible, *i.e.* for all systems but naphthalene (see the positions of the NO_3 attacks in Scheme 1). Actually keeping this constraint while the two moieties come closer leads to a radical adduct which is a conformational transition structure connecting two enantiomeric C_1 adducts. However, the energy differences resulted to be small (see Tables) and not relevant for the purpose of our study. Some geometrical constraints were also adopted in order to avoid the formation of complexes that are not relevant for our study and that lead to discontinuities in the potential energy curve (see the preliminary DFT scan in Figure 3 in the Supplementary Material)

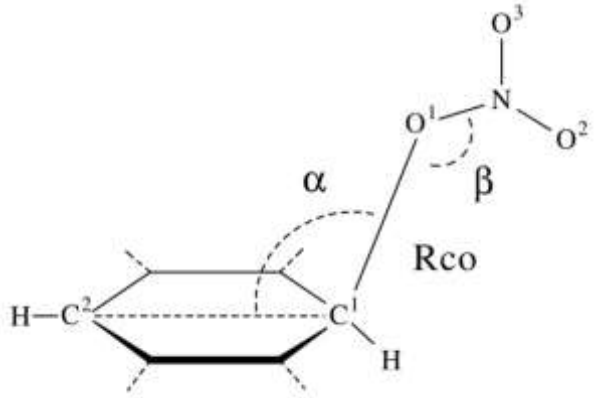

Scheme 3. The general structure: symmetry and geometric constraints (see text).

Scheme 3 shows the symmetry and geometrical constraints: C^2, C^1, O^1, N, O^2, and O^3 lie all on the plane that cuts the PAH molecule in two equivalent parts; angles α and β are kept fixed to the value optimized in the adduct. Rco is the C^1-O^1 distance subject to scan from 10.0 Å (7.0 Å for Naphthalene) to the bond distance in the adducts.

CASSCF/CASPT2 calculations have been performed with the program MolCAS 7.4.[53] The Cholesky decomposition has been used to speed up the calculation of two-electron integrals.[54] CBS-QB3 and DFT geometry optimizations have been performed with Gaussian 09.[55]

Results and Discussion.

Benzene. As for all other species subject of the present study, preliminary CBS-QB3, B3LYP/(A)DZ and single points CASPT2/(A)DZ calculations have been performed. For the latter only relevant C_s structures within the constraints described above are presented both in the Table and Figures. The active space was defined as (17,12), a combination of (6,5) for benzene and (11,7) for NO_3. Table 1 collects the data. More data can be found in the Supplementary Material.

Table 1. Benzene + nitrate radical: electronic energies (eV).

	Ionization[a]		Vertical	Adduct[c]		TS[d]	
	Vert.	Adiab.	E. T.[b]	C_S	C_1	C_S	C_1
CBS-QB3	9.54	9.41	5.57	-0.34	-0.41	0.01	-0.04
DFT	9.15	9.01	5.26	-0.09	-0.12	0.06	0.04
CASPT2	9.21	-[e]	6.23	0.03	-[e]	-[e]	-[e]

[a] Vertical and adiabatic ionization energies of benzene; [b] Vertical Electron Transfer energies from benzene to nitrate; [c] Radical adduct energies with (C_s) and without (C_1) symmetry constraint; [d] Addition Transition Structure energies with (C_s) and without (C_1) symmetry constraint; [e] Not calculated (see text).

The calculated ionization energies can be compared with the experimental value of 9.24 eV. More interesting are the values of the "Vertical Electron-Transfer", *i.e.* the energies required to ionize benzene generating the radical cation and the nitrate anion at their initial geometries. These range from 5.3 to 6.2 eV. The formation of the radical adduct is calculated to be slightly exoergic. The energy barriers are also quite low. From the free energies barriers at 298 K (see Supplementary Material) the following rate constants for the addition of NO_3 to benzene are calculated: CBS-QB3 5.4×10^{-14} cm^3 $molecule^{-1}$ s^{-1}, DFT 3.1×10^{-15} cm^3 $molecule^{-1}$ s^{-1} Both rate constants are overestimated with respect to the experimental value of $2.7 \div 6.2 \times 10^{-17}$ cm^3 $molecule^{-1}$ s^{-1} suggested by Atkinson.[56] Figure 1a shows the potential energy curves of the lowest four electronic states as a function of the CO distance. S_0 is the ground state; its energy at 10 Å is set to 0 eV and used as a reference for all other states and distances. S_1 and S_2 correspond to the excited state $^2E'$ of NO_3 (it is deduced by the occupation numbers of the active MOs); their energies at 10 Å are 2.07 and 2.14 eV and can be compared with the experimental value of 1.87 eV.[45] S_3 at 10 Å is the ET state. This can be deduced by the charge of the NO_3 group (~ -1.0) reported in Figure 1b while the

other states do not present any charge on NO_3. The dominant electronic configuration, describing an electron transition from a π orbital localized on benzene to the semi-occupied σ orbital localized on NO_3, confirms the ET nature of S_3. As expected, the energy of the ET state lowers as benzene (a radical cation in this state) and the NO_3 (as anion) get closer because of the coulomb attraction. This trend is very clear between 10 and 3.2 Å where the ET state keeps the negative charge on NO_3. The other states keep almost constant energies and null charges on NO_3. Around 3.1 Å the ET state and the two $^2E'_{NO3}$ states give rise to avoided-crossings between the CASPT2 curves. The CASSCF energy curves also come close (see Figure 1, Supplementary Material). The Electron Transfer character is transferred to the S_1 state. This behaviour is illustrated in Figure 1b: between 3.1 and 2.25 Å the charge of NO_3 drops from 0 to -0.3 in S_1 while it rises to the same value from ~-1 in S_3 (trace of this exchange also involve S_2). At 2.13 Å, where the ground state S_0 presents a maximum, the charges of the NO_3 group in the states S_1 and S_3 are around -0.2. At this point S_1, S_2 and S_3 have substantially changed their nature: they now correspond to excited states of the incipient radical adducts. This change generates serious convergence problems in the CASPT2 calculation known as "intruder states" problem that cannot be solved by techniques like imaginary shift.[38,39] These problems prevent the study of the excited states at shorter CO distances without extension of the active space beyond the computational feasibility. The maximum at 2.13 Å on the S_0 curve indicates the presence of the transition structure (whose exact localization is not the object of this study). The group charge of NO_3 in S_0, initially 0 e^- at 10 Å, starts to become negative at 3.2 Å and reaches the value of -0.44 in the radical adduct as a consequence of the electronegativity of the group. Therefore, from the observation of Figure 1 we can deduce that the attack of the NO_3 radical to benzene essentially follows a "radical pathway" (Scheme 2).

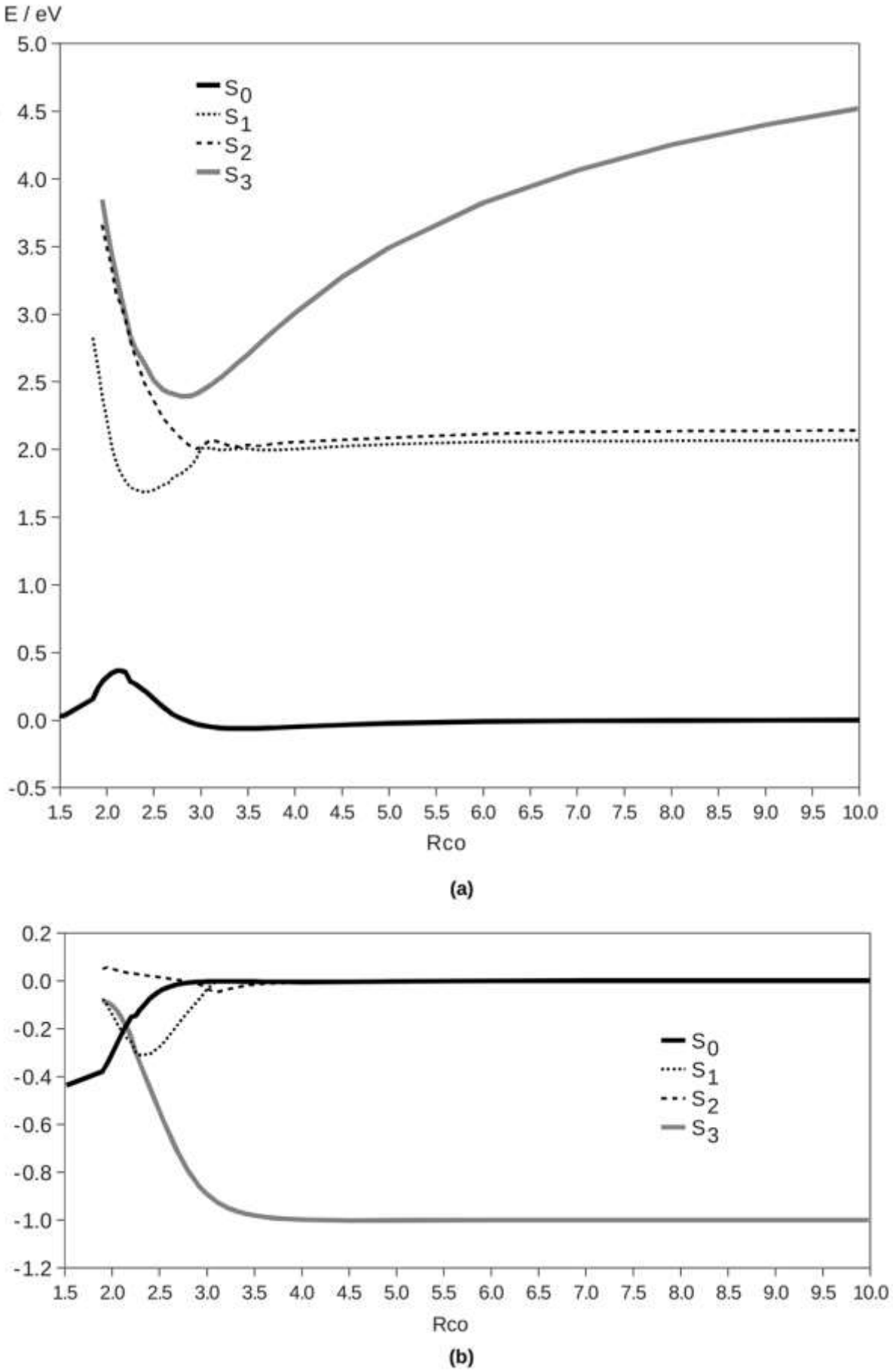

Figure 1. Benzene + NO_3: Four states CASPT2 potential energy curves (a) and electronic group charges of NO_3 (b) as a function of the CO distance (Rco, in Å).

Naphthalene. This molecule, the smallest PAH, is one of the most abundant environmental pollutants present in the troposphere. It can ionize more easily than benzene because its experimental IP is 8.14 eV, which can be compared with the values reported in Table 2. The Vertical Electron Transfer is calculated around 4 ÷ 4.6 eV, *i.e.* more than 1 eV lower than the value calculated for benzene. For the CASPT2 calculations, the active space was defined as (19,13), a combination of a (8,6) for napthhalene and (11,7) for NO_3.

Table 2. Naphthalene + nitrate radical: electronic energies (eV).

	Ionization[a]		Vertical	Adduct[c]	TS[d]
	Vert.	Adiab.	E. T.[b]		
CBS-QB3	8.28	8.18	4.30	-0.69	-0.21
DFT	7.84	7.75	3.95	-0.42	-0.23
CASPT2	7.96	-[e]	4.62	-0.48	-[e]

[a] Vertical and adiabatic ionization energies of naphthalene; [b] Vertical Electron Transfer energies from naphthalene to nitrate; [c] Radical adduct energies; [d] Addition Transition Structure energies; [e] Not calculated (see text).

The following rate constants for the addition of NO_3 to naphthalene are calculated: CBS-QB3 5.4×10^{-12} cm^3 $molecule^{-1}$ s^{-1}, DFT 8.7×10^{-12} cm^3 $molecule^{-1}$ s^{-1}. Both rate constants slightly overestimate the experimental value of 1.2×10^{-13} cm^3 $molecule^{-1}$ s^{-1} reported by Kwok *et al.*,[57] hence in better agreement than in the benzene case. In the reaction of NO_3 with naphthalene the lack of any symmetry forced us to include six electronic states in the CASPT2 study. Convergence problems due to *intruder states* prevented the study at very long CO distances: therefore, the potential energy and NO_3 group charge curves where calculated only up to 7 Å (Figure 2). S_0 is the ground state. The states S_1 and S_2 (calculated at 1.39 and 1.41 eV above S_0 at 7 Å) correspond to electronic excitations in the NO_3 group ($^2A_{NO3}$, hereafter). States S_3 and S_4 correspond to the $^2E'_{NO3}$ states (as in the Figure 1 for Benzene). S_5 is the ET state, as can be deduced from the NO_3 group charge (~ -1.0) reported in Figure 2b and by the dominant electronic configuration. For all other states the charge of NO_3 is zero. As naphthalene and NO_3 get closer, S_5 lowers its energy while the other states keep their energy almost constant and retain null charges on NO_3.

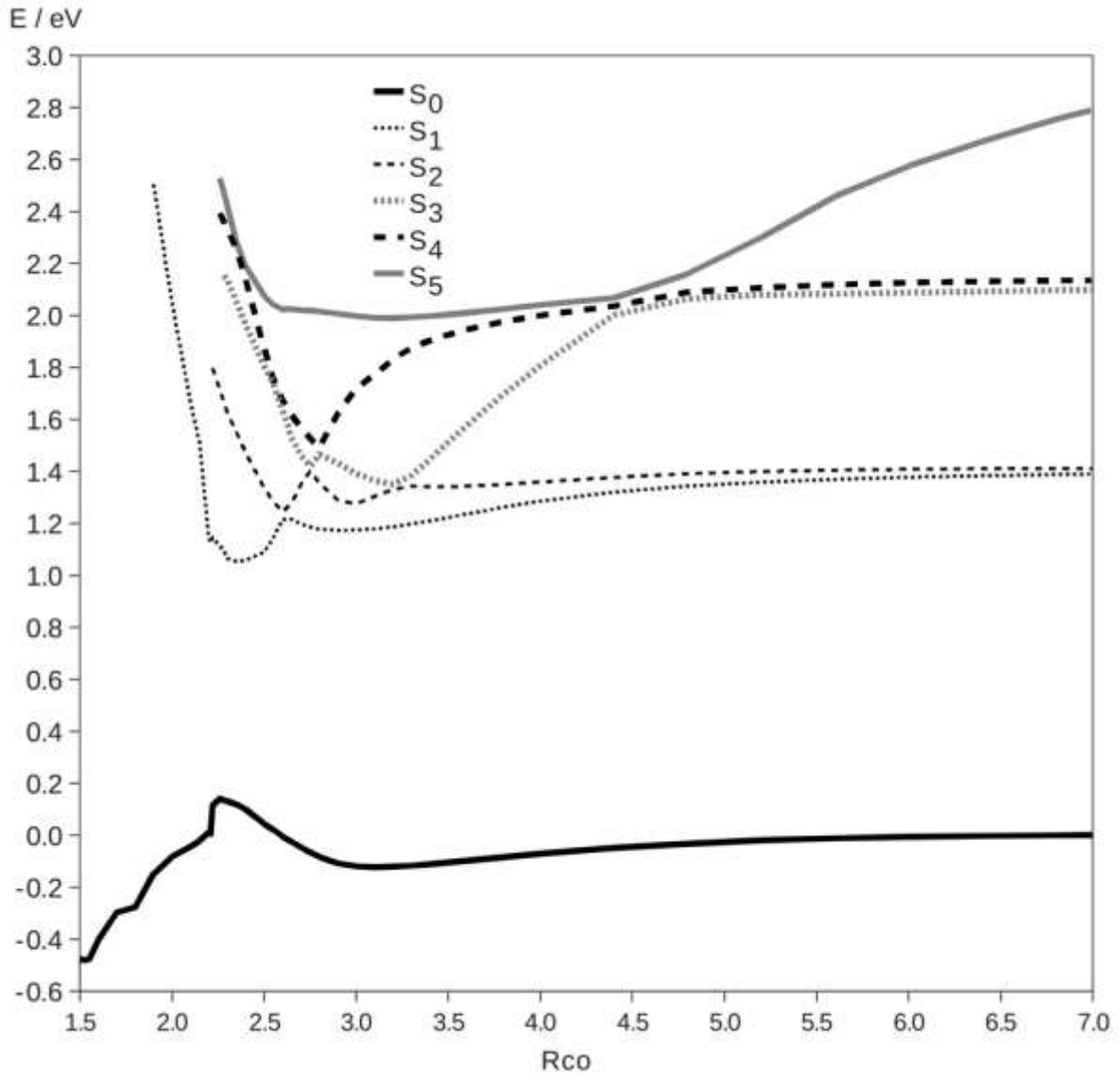

(a)

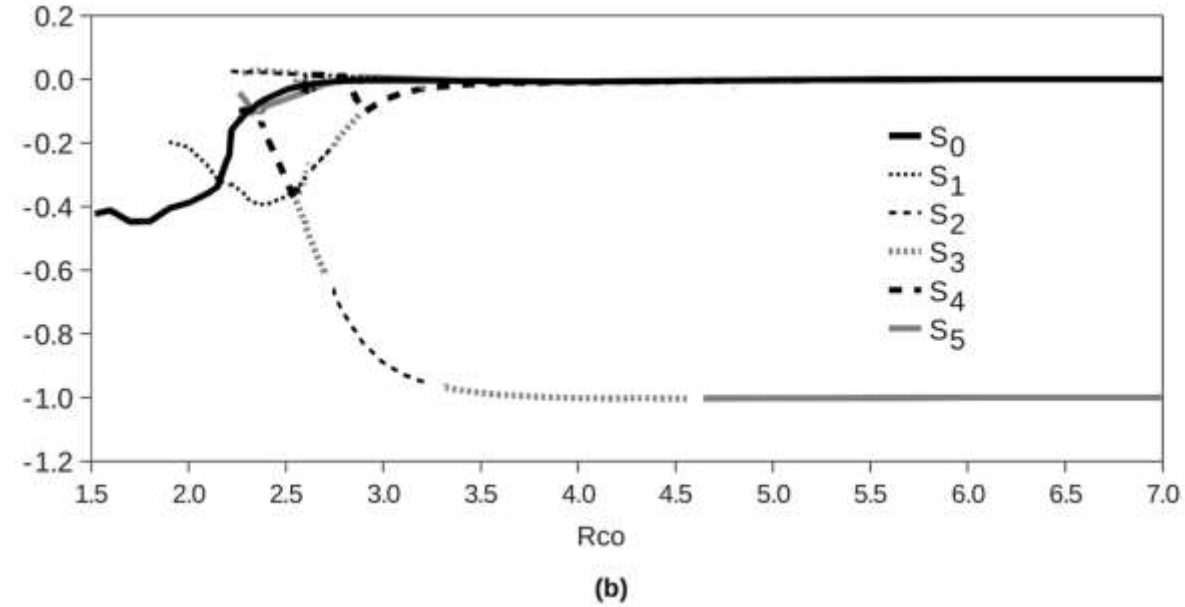

(b)

Figure 2. Naphthalene + NO_3: Six states CASPT2 potential energy curves (a) and electronic group charges of NO_3 (b) as a function of the CO distance (Rco, in Å).

Between 4.6 and 4.8 Å the ET state goes below the $^2E'_{NO3}$ states, so becoming the new S_3. This is evident by the energy trend shown in Figure 2a and by the negative charge on NO_3 which moves from S_5 to S_3 (Figure 2b). The null extra-diagonal elements[58] in the MultiState CASPT2 matrix (and the fact that the CASSCF curves do not cross being well separated, $\Delta E > 1$ eV, see Figure 2, Supplementary Material) suggest that these are real crossings. A crossing seam of two potential energy surfaces of the same symmetry involving ET states have already been observed since 1992.[59] Because of the lack of symmetry, deviations from the geometrical constraints should not change the nature of the crossing. Therefore, the ET state and the $^2E'_{NO3}$ states give rise to "*extended surface touching*".[60] Clearly, improvements of the wave-function (more MOs in the AS) and of the Hamiltonian (spin-orbit coupling[61]) will probably remove the degeneracies. However, the real nature of these crossings is not relevant for our study because we are mainly interested on the role of the ET state when NO_3 approaches to the PAH and its possible interaction with the ground state. The states labelling continue to follow their energy order. At CO distances below 3.3 Å several CASPT2 avoided-crossings take place with a transfer of the ET character to the lower excited states. At 2.4 Å, S_1 is now the state with the largest share of negative charge on NO_3. However, most of the ET nature is lost: the charge on NO_3 in now only -0.39. As in the case of benzene, at shorter CO distances all states have changed their initial nature and they now correspond to internal excitation on the incipient radical adduct. A maximum at 2.26 Å on the S_0 curve hints to the presence of a transition structure. The charges on NO_3 are now -0.13 on S_0 and -0.33 on S_1. The clear indications about the lack of any role for an Electron Transfer pathway for the attack on NO_3 to napththalene (and convergence problems) convinced us not to investigate this system any further.

Anthracene. After naphthalene, anthracene is one of the most important environmental PAH pollutants.[62,63] The oxidation pathways of the radical adduct formed by it upon attack by NO_3 has been recently subject of study of our group.[16] The dimensions of the adduct prevented the CBS-QB3 calculations without symmetry constraint. No transition structures for the addition of NO_3 were localized on the potential energy surfaces. This suggested the possibility of an alternative mechanism for the attack of NO_3, *i.e.*, the Electron Transfer pathway. The Vertical E.T. is calculated between 3.2 ÷ 3.9 eV. This value is more than 2 eV lower than that calculated for benzene and almost 1 eV lower than that calculated for naphthalene.

Table 3. Anthracene + nitrate radical: electronic energies (eV).

	Ionization[a]		Vertical	Adduct[c]		TS[d]	
	Vert.	Adiab.	E. T.[b]	C_S	C_1	C_S	C_1
CBS-QB3	7.54	7.42	3.56	-1.09	-[f]	-[f]	-[f]
DFT	7.04	6.97	3.15	-0.87	-0.87	-[f]	-[f]
CASPT2	7.22	-[e]	3.90	-0.95	-[e]	-[e]	-[e]

[a] Vertical and adiabatic ionization energies of anthracene; [b] Vertical Electron Transfer energies from anthracene to nitrate; [c] Radical adduct energies with (C_s) and without (C_1) symmetry constraint; [d] Addition Transition Structure energies with (C_s) and without (C_1) symmetry constraint; [e] Not calculated (see text); [f] Not found.

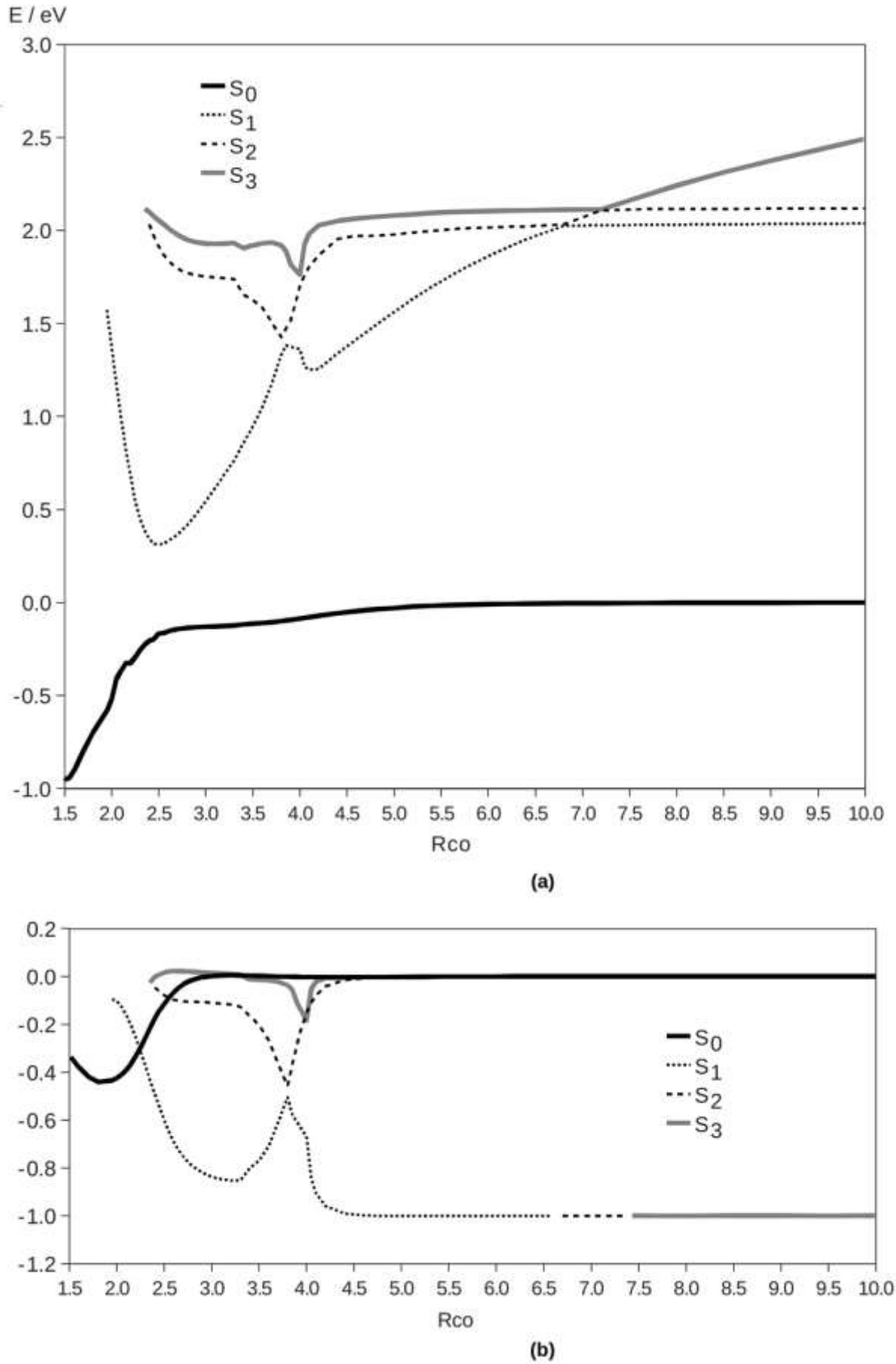

Figure 3. Anthracene + NO_3: Four states CASPT2 potential energy curves (a) and electronic group charges of NO_3 (b) as a function of the CO distance (Rco, in Å).

The attack to the central part of the PAH (see Scheme 1) allowed the use of the C_s symmetry constraint (as in benzene). Four states where sufficient for the CASPT2 calculations, the active space was defined as (19,13), a combination of a (8,6) for anthracene and (11,7) for NO_3. Figure 3 shows the energy curves (a) and the charges on NO_3 group (b) for all the states as function of the CO distance from 1.5 to 10 Å. As in the previous cases, S_0 is the ground state, whose energy at 10 Å is taken as a reference. The two states (S_1 and S_2) at 2.04 and 2.12 eV correspond to the excited state $^2E'$ of NO_3. S_3 is the ET state which is located at 2.49 eV. Around 7.2 Å, the ET state crosses the $^2E'_{NO3}$ states becoming the new S_1 state. Because these state already belong to the same irreducible representations A', breaking the symmetry should not change the nature of the crossing. Therefore, as for naphthalene, the ET state and the $^2E'_{NO3}$ states give rise to "*extended surface touching*". Between 3.7 and 4.1 Å, avoided crossings involving CASPT2 curves (see also Figure 4, Supplementary Material for the analogous CASSCF curves) take place as can be deduced by the energy curves and by the charge trends on NO_3. The state S_1 keeps its ET character. At 2.55 Å, where the S_1 and S_0 reach their minimal energy gap (0.48 eV), the former presents a charge on NO_3 of -0.65, while in S_0 the charge on NO_3 is only -0.09. At shorter distances, S_1 loses its ET character and its energy rapidly rises while the negative charge on NO_3 in S_0 becomes larger. As the CO distance gets closer, the S_0 curve declines without passing through any energy maximum. Therefore, we have a clear indication that the addition of NO_3 to anthracene takes place without a transition structure. Interestingly, the negative charge on NO_3 presents a minimum around 1.9 Å. In other words, along the approximate reaction coordinate (the CO distance) we found a point where the ground state presents a charge transfer character being the negative charge on NO_3 greater than that found in the radical adduct. For this reason, we decided to better explore the two lowest states (energy and NO_3 charge curves are shown in Figure 4) below 3.5 Å where S_1 is well separated from the other states and shows a clear ET character.

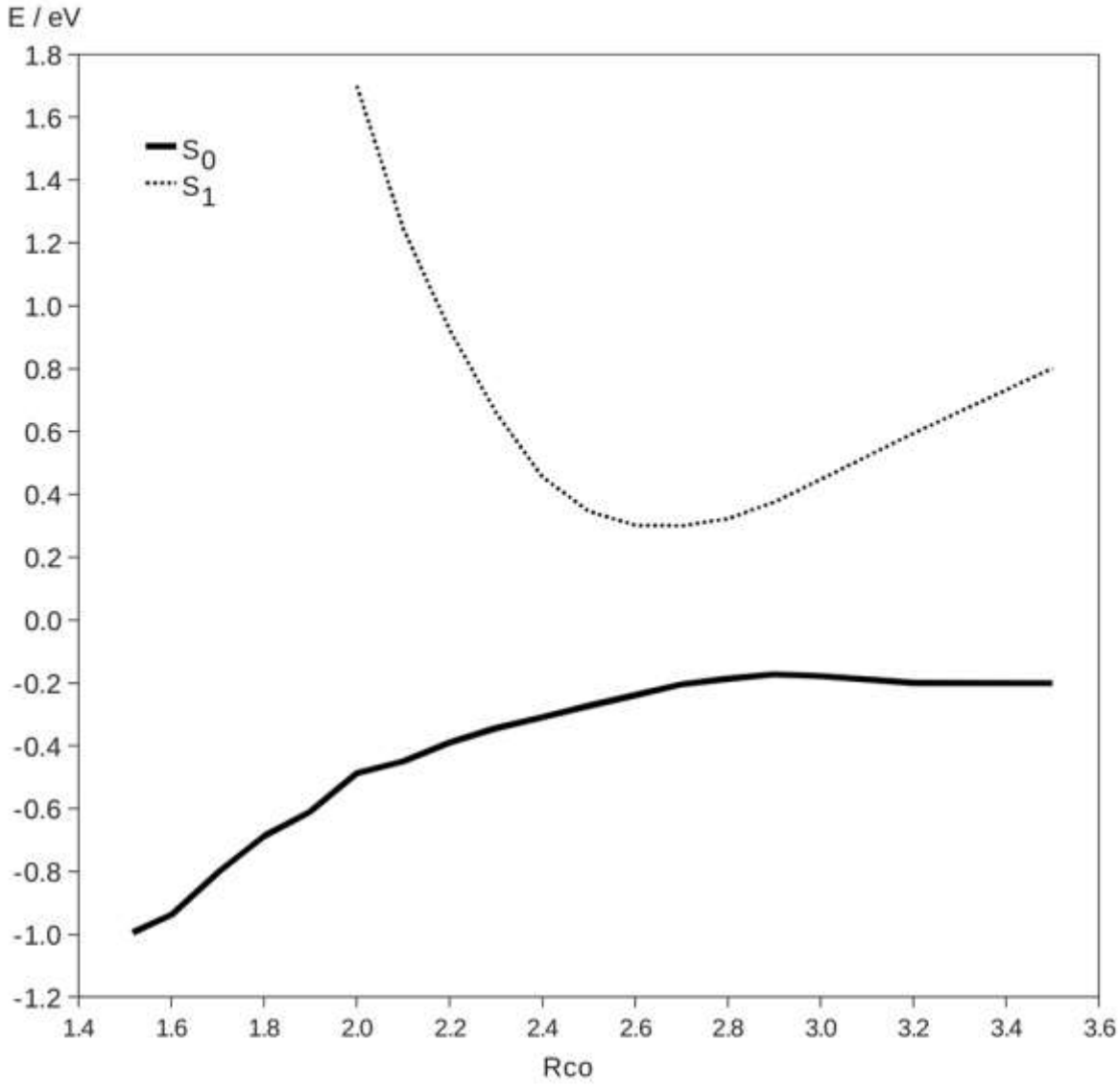

(a)

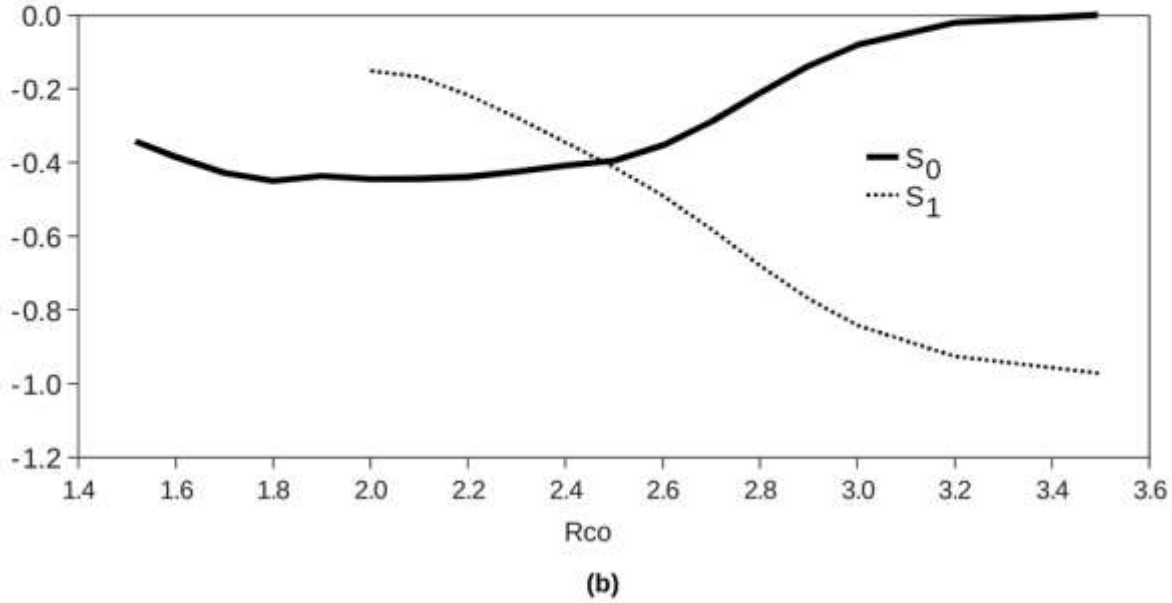

(b)

Figure 4. Anthracene + NO_3: Two states CASPT2 potential energy curves (a) and electronic group charges of NO_3 (b) as a function of the CO distance (Rco, in Å).

Figure 4 substantially confirms what we observed in the previous picture. The ground state curve does not show a clear maximum (some sort of bump appears but we must remember that these are CASPT2 calculations on DFT geometries). More interesting is the minimum (-0.45, Figure 4b) of the charge on NO_3 reached at 1.8 ÷ 2.2 Å that can be compared with value found for the radical adduct (-0.34). On the basis of these data, we can assess that the ground state NO_3 addition pathway to anthracene is endowed with partial ET character. This fact, along with the exoergicity of the reaction (the radical adduct is ca 1 eV *i.e.* 23 kcal mol^{-1} below the reactants) can explain the lack of a clear transition structure.

Pentacene. Proceeding along the acene family, the extension of the chain of fused benzene rings would lead to modelling the reaction of NO_3 with tetracene. However, the dimension of this system, and the lack of any exploitable symmetry for the attack of NO_3, prevent CASPT2 calculations. Therefore, the study was extended to pentacene, where the attack of NO_3 to the central position (see Figure 1) allows the use of the C_s symmetry constraint (as in the reaction with anthracene). The electronic properties are reported in Table 4.

Table 4. Pentacene + Nitrate radical: electronic energies (eV).

	Ionization[a]		Vertical	Adduct[c]		TS[d]	
	Vert.	Adiab.	E. T.[b]	C_S	C_1	C_S	C_1
CBS-QB3	6.54	6.48	2.56	-[e]	-[e]	-[e]	-[e]
DFT	6.11	6.06	2.21	-1.41	-1.43	-[f]	-[f]
CASPT2	6.41	-[e]	3.15	-1.38	-[e]	-[e]	-[e]

[a] Vertical and adiabatic ionization energies of Pentacene; [b] Vertical Electron Transfer energies from pentacene to Nitrate; [c] Radical adduct energies with (C_s) and without (C_1) symmetry constraint; [d] Addition Transition Structure energies with (C_s) and without (C_1) symmetry constraint; [e] Not calculated (see text); [f] Not found.

Due to the dimensions of the adduct, the CBS-QB3 calculations where not feasible even with the C_s symmetry constraint. Only DFT optimizations were possible and, as for anthracene, no transition structure for the addition of NO_3 to pentacene was localized. These facts explain why the last two columns of the table, reported for sake of homogeneity with the previous ones, are empty.

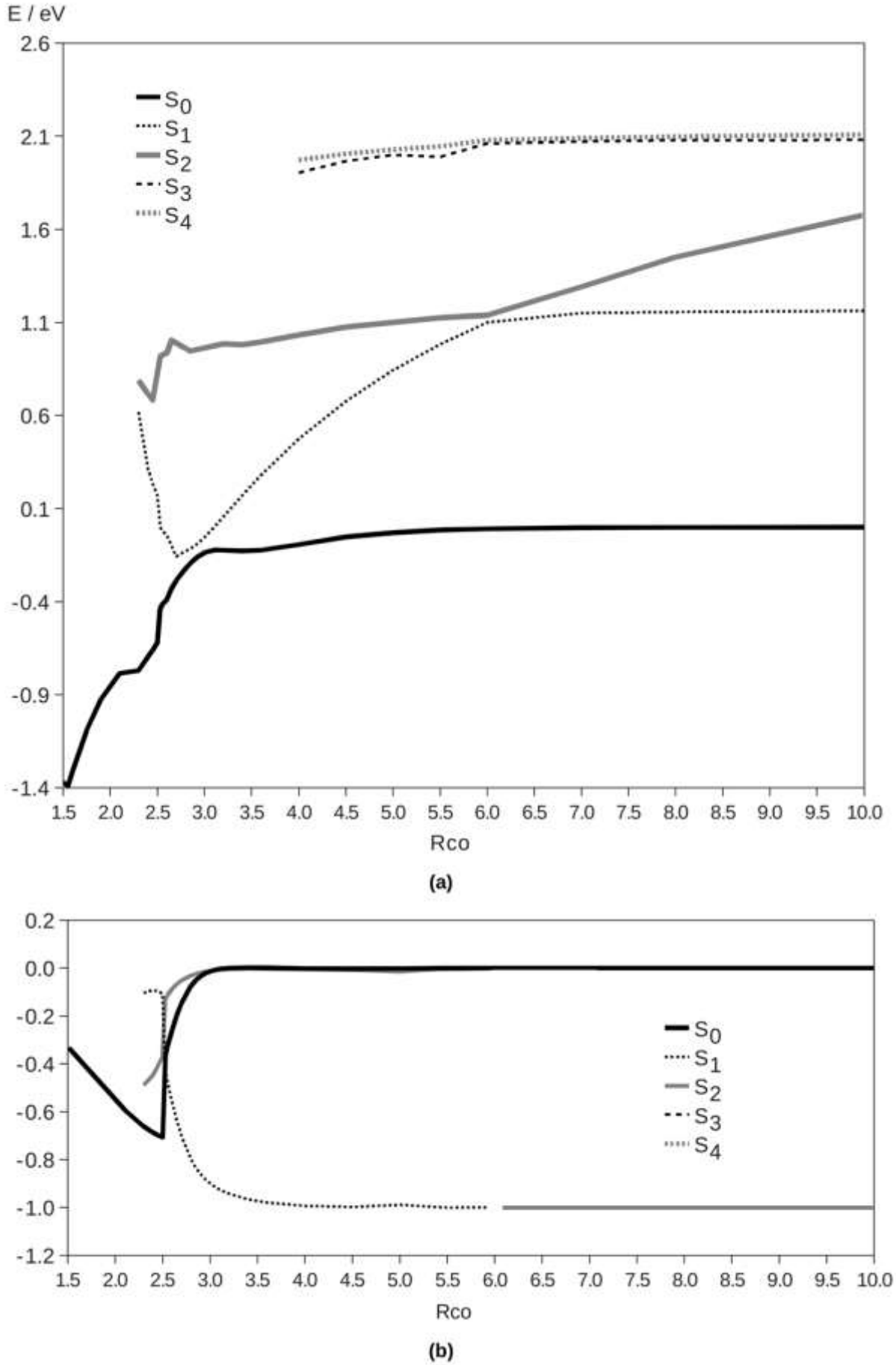

Figure 5. Pentacene + NO_3: Five states CASPT2 potential energy curves (a) and electronic group charges of NO_3 (b) as a function of the CO distance (Rco, in Å).

Despite the symmetry constraints, five states where required in the State Average calculation because of the presence of a ππ* excited state localized on the aromatics and encountered just above the ground state. The active space was defined as (19,13), a combination of a (10,7) for pentacene and (9,6) for NO_3. Energy curves and the charges on the NO_3 group for all states as function of the CO distance from 1.5 to 10 Å are shown in Figure 5. S_0 is the ground state whose energy at 10 Å used again as a reference. S_1 corresponds to the ππ* excited state localized on the aromatics. S_2 is the ET state which is located at 1.68 eV. The two states (S_3 and S_4) at 2.08 and 2.11 eV correspond to the excited state $^2E'$ of NO_3. We must stress that the inclusion of these two states in the calculations is compulsory because at the CASSCF level the ET state is above these states. As for all other cases, the ET state lowers its energy as the pentacene and NO_3 get closer. Around 6.0 Å, the ET state crosses the ππ* state becoming the new S_1 state ("*extended surface touching*" as in the case of anthracene). Around 3.0 Å S_0 and S_1 show an avoided crossing: the ground state suddenly starts to stabilize and the NO_3 group gets the negative charge; the first excited state energy rapidly rises and NO_3 group loses its charge. At shorter CO distances, convergence problems due to *intruder states* give raise to discontinuities on the curves.

As for anthracene, the main role of the two first electronic states allowed us to repeat the calculation with this smaller number of state in the State-Average calculations. Figure 6 shows the energy curves (a) and the charges on NO_3 group (b) for S_0 and S_1 as function of the CO distance from 1.5 to 4.5 Å. The result is clear: between 3.4 and 3.8 Å (0.2 – 0.6 Å more than the sum of the van der Waals radius) a sort of electron transfer from pentacene to NO_3 takes place; in the ground state the NO_3 starts to become an anion while in the first excited state NO_3 loses its negative charge. At 3.0 Å (0.2 Å below the sum of the van der Waals radius but 1.5 Å longer than the bond distance) the group NO_3 in S_0 shows a charge of -0.84, *i.e.* the ground state is essentially constituted by a pentacene radical cation plus a nitrate anion. This electronic structure is a consequence of the high weight (83%) of the charge-transfer configurations in the electronic ground state. This behaviour is quite similar to that observed in the case of LiF[27]. As the CO bond is formed, the negative charge on NO_3 declines until it reaches the smaller value assumed in the radical adduct (-0.33), which is due to the electronegativity of the group. Therefore, although the NO_3 moiety never reaches a unitary negative charge, this is in any case significantly greater than that assumed in the final

adduct. Because the phenomenon takes place at a relatively short CO distance, we can assess that pentacene reacts with NO_3 radical following a sort of *inner-sphere* Electron Transfer pathway.

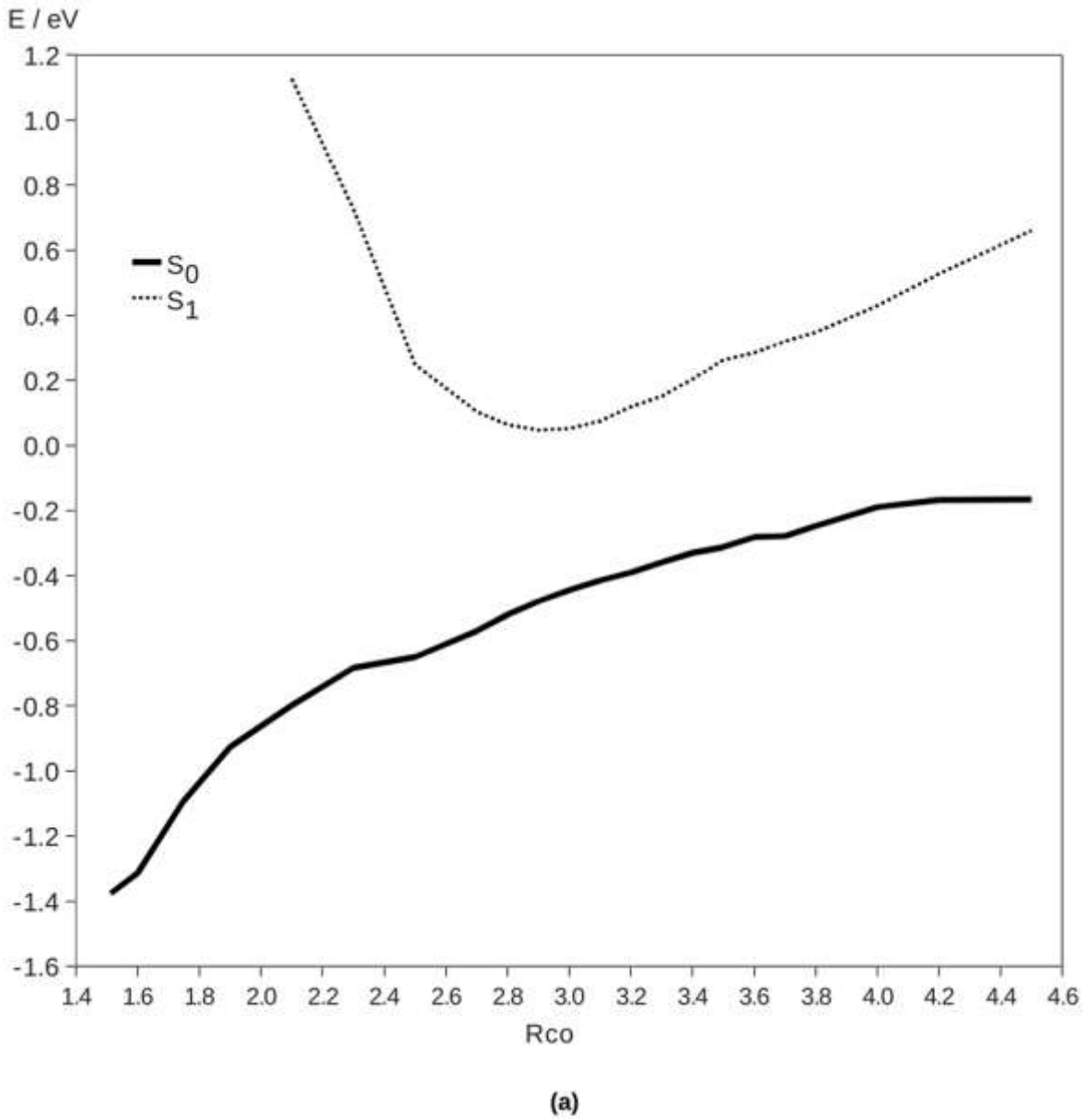

(a)

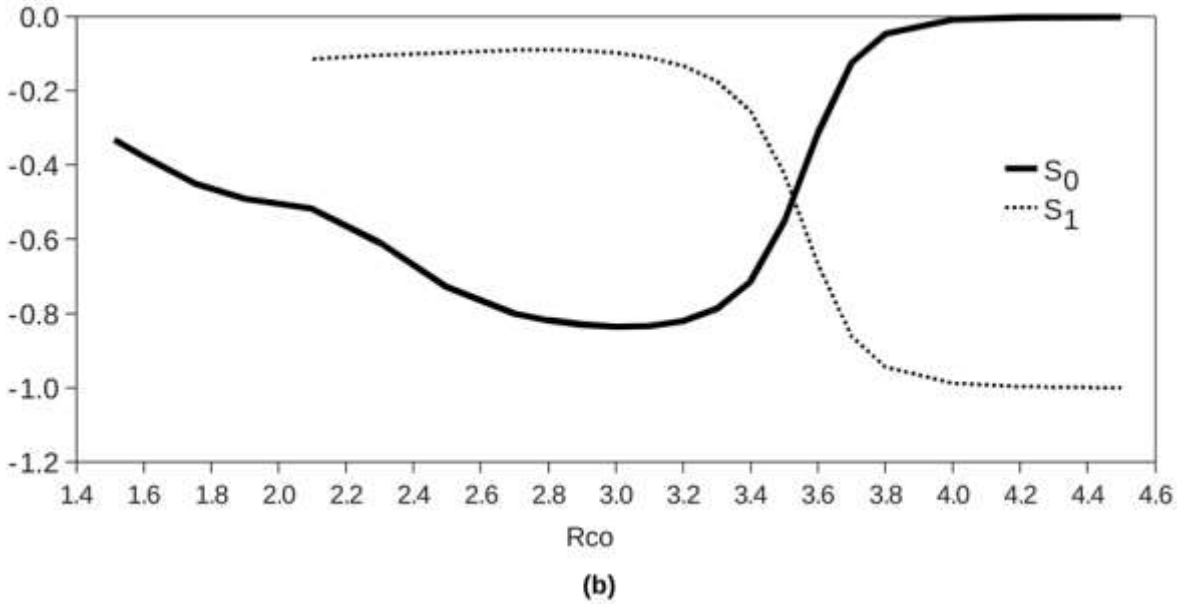

(b)

Figure 6. Pentacene + NO_3: Two states CASPT2 potential energy curves (a) and electronic group charges of NO_3 (b) as a function of the CO distance (Rco, in Å).

Conclusions.

The addition of the radical NO_3 (electron affinity 3.94 eV) to some selected acenes, (Scheme 1) follows different mechanisms depending on the dimension of the PAH, hence on its ionization potential, IP. Benzene and naphthalene, whose ionization potentials are at least 8 eV, react with a "normal" radical mechanism. Anthracene (IP ~7.4 eV) also seems to react mainly in this way. However, the addition pathway is characterized by some electron transfer trait. By contrast, pentacene (IP ~6.9 eV) reacts with a sort of *inner-sphere* Electron Transfer mechanism: when the two approaching species reach a distance of ca. 3.5 Å, the system assumes a strong character of ET, generating the couple "pentacene radical cation plus nitrate anion". As soon as this occurs, the coulomb attraction is effective in binding the two species. As a consequence, it generate the radical adduct without any (electronic) energy barrier. These results indicate that PAHs with 4/5 or more fused benzene rings and whose ionization potential is below ca. 7 eV, will react following the Electron Transfer mechanism entailing high rate constants. This result could be important in the study of the degradation of PAH in the gas-phase environment. The presence of a polar solvent could favour the formation of the two ions, thus leading to an extension of the role of the Electron Transfer pathway to smaller PAHs.

Supplementary Material. It includes tables with electronic energies of critical points at DFT, CBS-QB3 and CASPT2 level; tables of electronic energies and reference weights for all SA-CASSCF and CASPT2 states as a function of the CO distance; figures of the electronic energies for all SA-CASSCF and CASPT2 states as a function of the CO distance; figures of the MOs in the AS for NO_3 at 10 Å.

Acknowledgements. This work was sustained by Università di Torino (GHIG_RILO_16_02).

References.

1. B. J. Finlayson-Pitts, J. N Pitts, J. N., 2000. Chemistry of the Upper and Lower Atmosphere, in: Press, A. (Ed.), Chemistry of the Upper and Lower Atmosphere. Elsevier, pp. 436–546.

2. I. J. Keyte, R. M. Harrison and G. Lammel, *Chem. Soc. Rev.* **2013**, *42*, 9333–9391. doi:10.1039/c3cs60147a

3. L. H. Lim, R. M. Harrison and S. Harrad, *Environ. Sci. Technol.* **1999**, *33*, 3538–3542. doi:10.1021/es990392d
4. B. M. Jenkins, A. D. Jones, S. Q. Turn and R. B. Williams, *Environ. Sci. Technol.* **1996**, *30*, 2462–2469. doi:10.1021/es950699m
5. M. Mandalakis, Ă. Gustafsson, T. Alsberg, A.-L. Egeback, C. M. Reddy, L. Xu, J. Klanova, I. Holoubek, E. G. Stephanou, *Environ. Sci. Technol.* **2005**, *39*, 2976–2982. doi:10.1021/es048184v
6. V. Samburova, J. Connolly, M. Gyawali, R. L. N. Yatavelli, A. C. Watts, R. K. Chakrabarty, B. Zielinska, H. Moosmaźller and A. Khlystov, *Sci. Total Environ.* **2016**, *568*, 391–401. doi:10.1016/j.scitotenv.2016.06.026
7. N. Asare, N. E. Landvik, D. Lagadic-Gossmann, M. Rissel, X. Tekpli, K. Ask, M. Låg and J. A. Holme, *Toxicol. Appl. Pharmacol.* **2008**, *230*, 175–186. doi:10.1016/j.taap.2008.02.015
8. N. Asare, X. Tekpli, M. Rissel, A. Solhaug, N. Landvik, V. Lecureur, N. Podechard, G. Brunborg, M. Lag, D. Lagadic-Gossmann and J. A. Holme, *Mutagenesis* **2009**, *24*, 481–493. doi:10.1093/mutage/gep032
9. J. L. Durant, W. F. Busby, A. L. Lafleur, B. W. Penman and C. L. Crespi, *Mutat. Res. Toxicol.* **1996**, *371*, 123–157. doi:10.1016/s0165-1218(96)90103-2
10. N. Landvik, M. Gorria, V. Arlt, N. Asare, A. Solhaug, D. Lagadic-Gossmann and J. Holme, *Toxicology* **2007**, *231*, 159–174. doi:10.1016/j.tox.2006.12.009
11. G. Talaska, P. Underwood, A. Maier, J. Lewtas, N. Rothman and M. Jaeger, *Environ. Health Perspect.* **1996**, *104*, 901–906. doi:10.2307/3433008
12. D. Stone, M. J. Evans, H. Walker, T. Ingham, S. Vaughan, B. Ouyang, O. J. Kennedy, M. W. McLeod, R. L. Jones, J. Hopkins, S. Punjabi, R. Lidster, J. F. Hamilton, J. D. Lee, A. C. Lewis, L. J. Carpenter, G. Forster, D. E. Oram, C. E. Reeves, S. Bauguitte, W. Morgan, H. Coe, E. Aruffo, C. Dari-Salisburgo, F. Giammaria, P. Di Carlo and D. E. Heard, *Atmos. Chem. Phys.* **2014**, *14*, 1299–1321. doi: 10.5194/acp-14-1299-2014
13. X. Qu, Q. Zhang and W. Wang, *Chem. Phys. Lett.* **2006**, *426*, 13–19. doi: 10.1016/j.cplett.2006.05.070
14. X. Qu, Q. Zhang and W. Wang. *Chem. Phys. Lett.* **2006**, *432*, 40–49. doi: 10.1016/j.cplett.2006.10.041
15. G. Ghigo, M. Causà, A. Maranzana and G. Tonachini, *J. Phys. Chem. A* **2006**, *110*, 13270–13282. doi: 10.1021/jp064459c
16. A. Maranzana, G. Ghigo and G. Tonachini, *Atmos. Environ.* **2017**, *167*, 181–189. doi: 10.1016/j.atmosenv.2017.08.011
17. Y. Wang, B. Yang, J. Shu, N. Li, P. Zhang and W. Sun *Chem. Phys. Letters* **2015**, *635*, 146–151. doi:10.1016/j.cplett.2015.06.056
18. NIST http://webbook.nist.gov/cgi/cbook.cgi?ID=C12033497&Mask=20#ref-1 Web page consulted on November 2016.
19. NIST http://webbook.nist.gov/cgi/cbook.cgi?ID=C71432&Units=SI&Mask=20#Ion-Energetics Web page consulted on November 2016.
20. NIST http://webbook.nist.gov/cgi/cbook.cgi?ID=C91203&Units=SI&Mask=20#Ion-Energetics. Web page consulted on November 2016.

21. NIST http://webbook.nist.gov/cgi/cbook.cgi?ID=C120127&Units=SI&Mask=20#Ion-Energetics Web page consulted on November 2016.
22. NIST http://webbook.nist.gov/cgi/cbook.cgi?ID=C135488&Units=SI&Mask=20#Ion-EnergeticsWeb page consulted on November 2016.
23. P. Neta, R. E. Hu, *J. Phys. Chem.* **1986**, *90*, 4644–4648. doi:10.1021/j100410a035
24. Z. B. Alfassi, S. Padmaja, P. Neta and R. E. Huie, *J. Phys. Chem.* **1993**, *97*, 3780–3782. doi: 10.1021/j100117a025
25. D. G. Truhlar, in *The Encyclopedia of Physical Science and Technology*, 3rd ed., Edited by R. A. Meyers (Academic Press, New York, 2001), Vol. 13, pages 9-17.
26. F. Bernardi, M. Olivucci and M. A. Robb, *Chem. Soc. Rev.* **1996**, *25*, 321–328. doi: 10.1039/CS9962500321
27. C. W. Bauschlicher, S. R. Langhoff, *J. Chem. Phys.* **1988**, *89*, 4246–4254. doi: 10.1063/1.455702
28. H. Nakano, *J. Chem. Phys.* **1993**, *99*, 7983–7992. doi: 10.1063/1.465674
29. J. Finley, P.-Å. Malmqvist, B. O. Roos, and L. Serrano-Andrés, *Chem. Phys. Lett.* **1998**, *288*, 299–306. doi: 10.1016/S0009-2614(98)00252-8
30. F. Spiegelmann and J. P. Malrieu, *J. Phys.B: At. Mol. Phys.* **1984**, *17*, 1235–1257.
31. F. Spiegelmann and J. P. Malrieu, *J. Phys.B: At. Mol. Phys.* **1984**, *17*, 1259–1279.
32. P.-Å. Malmqvist, A. Rendell and B. O. Roos, *J. Phys. Chem.* **1990**, *94*, 5477–5482. doi: 10.1021/j100377a011
33. B. O. Roos, P. R. Taylor and P. E. M. Siegbahn, *Chem. Phys.* **1980**, *48*, 157–173. doi: 10.1016/0301-0104(80)80045-0
34. B. O. Roos, *Advances in Chemical Physics; Ab Initio Methods in Quantum Chemistry* (Ed.: K. P. Lawley), John Wiley & Sons Ltd., Chichester, 1987, vol. II, chapter 69. ISBN: 0-470-14294-4.
35. K. Andersson, P.-Å. Malmqvist, B. O. Roos, A. J. Sadley and K. J. Wolinski, *Phys. Chem.* **1990**, *94*, 5483–5488. doi: 10.1021/j100377a012
36. K. Andersson, P.-Å. Malmqvist and B. O. Roos, *J. Chem. Phys.* **1992**, *96*, 1218–1226. doi: 10.1063/1.462209
37. G. Ghigo, B. O. Roos and P.-Å. Malmqvist, *Chem. Phys. Lett.* **2004**, *396*, 142–149. doi: 10.1016/j.cplett.2004.08.032
38. M. Merchán, L. Serrano-Andrés, Ab Initio Method for Excited States. In *Computational Photochemistry*, 1st ed.; M. Olivucci, Ed.; Elsevier: Amsterdam, 2005; Vol. 16, pp 35−91.
39. M. Schreiber, M. Silva-Junior, S. Sauer and W. Thiel, *J. Chem. Phys.* **2008**, *128*, 134110. doi: 10.1063/1.2889385.
40. J. P. Zobel, J. J. Nogueira and L. Gonzalez, *Chem. Sci.*, **2017**, ***8***, 1482–1499. doi: 10.1039/c6sc03759c
41. T. H. Dunning *J. Chem. Phys.* **1989**, *90*, 1007–1023. doi: 10.1063/1.456153
42. V. Veryazov, P.-Å. Malmqvist and B. O. Roos, *Int. J. Quantum Chem.*, **2011**, *111*, 3329–3338. doi: 10.1063/1.4922352
43. K. Andersson, B.O. Roos, in: D.R. Yarkony (Ed.), *Modern Electronic Structure Theory, Part II*, World Scientific Publishing Co., Singapore, 1995. Par. 3.4.
44. W. Eisfeldand and K. Morokuma, *J. Chem. Phys.* **2000**, *113*, 5587–5587. doi:

10.1063/1.1290607
45. W. Eisfeld and K. Morokuma, *J. Chem. Phys.* **2001**, *114*, 9430–9440. doi: 10.1063/1.1370065
46. H. Xiao, S. Maeda and K. Morokuma, *J. Chem. Theory Comput.* **2012**, *8*, 2600–2605. doi: 10.1021/ct3004035
47. R. G. Parr, W. Yang, *Density Functional Theory of Atoms and Molecules*, Oxford University Press: New York, 1989; Ch.3; ISBN 0-19-509276-7
48. W. Jensen *Introduction to Computational Chemistry*, Wiley; Chichester, 1999, Chap. 6 ISBN 0-471-98425-6.
49. A. D. Kohn, A. D. Becke and R. G. Parr, *J. Phys. Chem.* **1996**, *100*, 12974–12980. doi:10.1021/jp960669l
50. A. D. Becke, *J. Chem. Phys.* **1993**, *98*, 5648–5652. doi: 10.1063/1.464913
51. C. Lee, W. Yang and R. G. Parr, *Phys. Rev. B* **1988**, *37*, 785–789. doi: 10.1103/PhysRevB.37.785
52. J. A. Montgomery Jr, M. J. Frisch, J. W. Ochterski and G. A. Petersson, *J. Chem. Phys.* **1999**, *110*, 2822–2827. doi: 10.1063/1.477924
53. F. Aquilante, L. De Vico, N. Ferré, G. Ghigo, P.-Å. Malmqvist, P. Neogrády, T. B. Pedersen, M. Pitoňák, M. Reiher, B. O. Roos, L. Serrano-Andrés, M. Urban, V. Veryazov and R. Lindh *J. Comput. Chem.* **2010**, *31*, 224–247. doi: 10.1002/jcc.21318
54. F. Aquilante, T. B. Pedersen and R. Lindh, *Theor. Chem. Acc.* **2009**, *124*, 1–10. doi: 10.1007/s00214-009-0608-y
55. Gaussian 09, Revision A.01, M. J. Frisch, *et al.* Gaussian, Inc., Wallingford CT, 2009.
56. R. Atkinson *J. Phys. Chem. Ref. Data* **1991**, *20*, 459–507.
57. E. S. C. Kwok, R. Atkinson and J. Arey, *Int. J. Chem. Kin.* **1994**, *26*, 511–525. doi: 10.1002/kin.550260504
58. E. Teller, *J. Phys. Chem.* **1937**, *41*, 109–116. doi: 10.1021/j150379a010
59. R. M. Manaa and D. R. Yarkony, *J. Chem Phys.* **1992**, *97*, 715–717. doi: 10.1063/1.1378324
60. N. J. Turro, V. Ramamurthy and J. C. Scaiano, *Principles of Molecular Photochemistry: An Introduction*, University Science Books, California, 2009, Ch. 6; ISBN 978-1-891389-57-3
61. S. Matsika and D. R. Yarkony, *J. Chem. Phys.* **2001**, *115*, 2038–2050. doi:10.1063/1.1378324
62. J. T. Andersson and C. Achten, *Polycycl. Aromat. Compd.* **2015**, *35*, 330–354. doi:10.1080/10406638.2014.991042
63. G. Lammel, *Polycycl. Aromat. Compd.* **2015**, *35*, 316–329. doi: 10.1080/10406638.2014.931870

Graphical Abstract

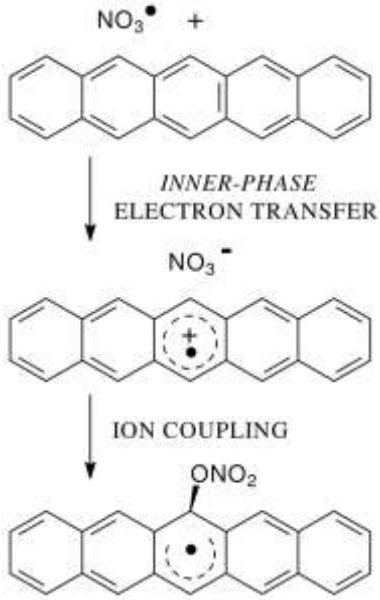

Mechanistic dichotomy in the addition of NO_3 to PAHs: The gas-phase reaction of radical NO_3 proceeds with radical mechanism with PAHs up to 3/4 fused rings while with the PAHs with 5 or more fused benzene rings the reaction follows an *inner-phase* Electron Transfer mechanism entailing high rate constants.